Atomic and Electronic Structure of Pyridine on Ge(100)

Suklyun Hong,*,† Young Eun Cho,‡ Jae Yeol Maeng,‡ and Sehun Kim*,‡

Department of Physics and Institute of Fundamental Physics, Sejong University, Seoul 143-747, Republic of Korea, and Department of Chemistry and School of Molecular Science (BK21), Korea Advanced Institute of Science and Technology, Daejon 305-701, Republic of Korea

Received: April 11, 2004; In Final Form: June 26, 2004

We have performed ab initio pseudopotential calculations in order to investigate the atomic and electronic structure of pyridine adsorbed on the Ge(100) surface. A large number of pyridine/Ge(100) adsorption configurations possibly resulting from cycloadditions and Lewis acid−base reactions are presented. The configuration having the Ge−N linkage formed by dative bonding with adsorbed pyridine molecules tilted is the most stable, which explains the experimental STM images well. The dative bonding character is investigated by comparing the charge densities for the clean and pyridine-adsorbed Ge(100) surfaces. Finally the difference between the Ge(100) and Si(100) surfaces is discussed.

Introduction

For the application of molecule-based devices, biosensors, and bio MEMS, functionalization of semiconductor surfaces through chemisorption of organic molecules becomes an interesting problem.[1−5] Because of their lone-pair electrons, molecules containing nitrogen such as pyridine (C_5NH_5), pyrimidine ($C_4N_2H_5$), and purine ($C_5N_4H_5$) have attracted particular attention; especially, the amine group can be used for the attachment of biomolecules such as DNA to the surface.[6] One of the prototypes for the organic functionalization is pyridine-chemisorbed Ge(100) surface. Pyridine is a tertiary amine with an aromatic ring. A pyridine molecule with two different functional groups can be attached to the Ge(100) surface via two different reaction types, cycloaddition and Lewis acid−base reactions.[1,7]

Cycloaddition reactions such as [2 + 2] or [4 + 2] cycloaddition are widely used in organic synthesis and are characterized by the creation of new σ bonds between at least two component molecules having π electrons to form a cyclic product. If the analogy made between traditional alkenes and the Si(100)-2×1 and Ge(100)-2×1 surface dimers holds, then cycloaddition surface products are likely to be observed on those surfaces: Many such examples have been indeed observed.[1]

Dative bonding, also known as coordinate covalent bonding, occurs when one molecule donates both of the electrons needed to form a sort of covalent bond.[1] One of the best known examples of dative bonding in chemistry is the reaction between ammonia (NH_3) and boron trifluoride (BF_3).[7] In this Lewis acid−base reaction, BF_3, known as the electrophile, serves as a Lewis acid and ammonia, the nucleophile, serves as a Lewis base. On Si(100)-2×1 or Ge(100)-2×1, such Lewis acid−base reactions are possible because of the zwitterionic nature of the buckled surface dimer. The functional groups with nonbonding electrons contain lone pairs and serve as a Lewis base to form a dative bond with the down atom of the surface dimer.[8−10]

Previously, we reported study of the formation of highly ordered pyridine molecules on Ge(100),[11] where only the key theoretical results necessary for the interpretation of our STM results are presented. Here we present the detailed theoretical results of the atomic and electronic structure for the pyridine molecules of 0.25 monolayers (ML) [one molecule per surface atom] adsorbed on Ge(100). Among many adsorption configurations for pyridine/Ge(100), the dative bonding configuration with adsorbed pyridine molecules tilted is found to be the most stable. The theoretical STM images for the most favorable model is compared with the experimental ones. The calculation methods are described in the next section, and results and discussion are followed.

Calculations

To investigate the configuration of pyridine on the Ge(100) surface we have performed ab initio calculations within the local density approximation (LDA) using the Vienna ab initio simulation package (VASP).[12,13] The atoms are represented by ultrasoft pseudopotentials as provided with VASP.[14] We used a kinetic energy cutoff of 224.5 eV. In the surface calculation, the theoretical lattice constant (5.634 Å) of germanium is used, which is in good agreement with the experimental value (5.658 Å). The pyridine-adsorbed Ge(100) surface is modeled by a slab with a $c(4\times2)$ surface supercell which is composed of a pyridine molecule (0.25 ML), six Ge layers, and an H layer passivating the bottom surface. The atomic positions at the two bottom Ge layers and the H layer are kept fixed, while the other layers are relaxed with residual forces smaller than 0.01 eV/Å. For the Brillouin-zone integration we use a 4 × 4 × 1 grid in the Monkhorst−Pack special point scheme. A Gaussian broadening with a width of 0.02 eV was used to accelerate the convergence in the *k*-point sum.

We simulate the constant-current STM images, with the use of the self-consistent Kohn−Sham eigenvalues and wave functions. The tunneling current $I(\mathbf{r}, V)$ is proportional to the energy-integrated local density of states weighted by a barrier transmission coefficient $T(E, V)$,[15,16] which reflects the change in the tunneling probabilty depending on E and V:

$$I(\mathbf{r}, \pm V) \propto \pm\sum_{n\mathbf{k}}\int_{E_F}^{E_F\pm V}|\psi_{n\mathbf{k}}(\mathbf{r})|^2\delta(E - E_{n\mathbf{k}})T(E, \pm V)\mathrm{d}E$$

$$\approx \pm\sum_{n\mathbf{k}}\int_{E_F}^{E_F\pm V}|\psi_{n\mathbf{k}}(\mathbf{r})|^2\delta(E - E_{n\mathbf{k}})\mathrm{d}E$$

* Corresponding authors: hong@sejong.ac.kr, sehkim@mail.kaist.ac.kr.
† Sejong University.
‡ Korea Advanced Institute of Science and Technology.

10.1021/jp048408w CCC: $27.50
Published on Web 08/25/2004

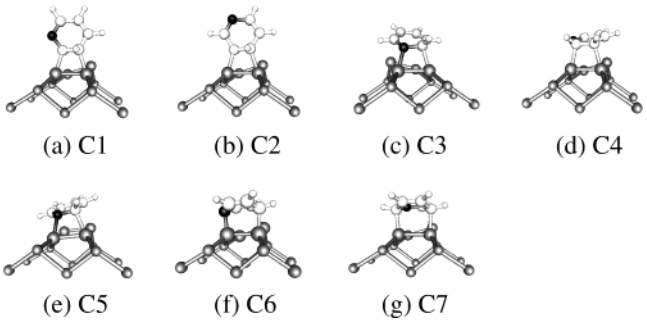

Figure 1. Optimized configurations with the $c(4\times2)$ surface unit cell at the 0.25 ML pyridine coverage for the [2 + 2] and [4 + 2] cycloaddition reactions between pyridine molecules and Ge dimers of Ge(100): (a−e) [2 + 2] and (f−g) [4 + 2]. White, black, and gray balls represent C, N, and Ge atoms, respectively, while hydrogen atoms are represented by small white balls.

where the second relation is obtained by the Tersoff−Hamann approximation,[17] and $+V$ and $-V$ represent the sample bias voltages for empty-state and filled-state measurements, respectively.

Results and Discussion

When the pyridine molecule is adsorbed on the Ge(100) or Si(100) surface, there are at least two possible reaction types for the chemisorption of pyridine due to its two different functional groups. One is cycloaddition between π-conjugated aromatic ring and Ge dimer. The other is a Lewis acid−base reaction resulting in dative bonding, in which the lone-pair electrons of pyridine are donated into the electron-deficient down-Ge atom in a Ge dimer. If pyridine molecules are covalently bonded to Ge(100) surface through [2 + 2] or [4 + 2] cycloaddition, the pyridine molecules will be located on the top of the Ge dimers, and the Ge dimers will be symmetric. If, on the other hand, adsorption occurs via Lewis acid−base reaction, the electron-rich up-Ge atom maintains the buckled-up state even after adsorption of pyridine molecules, so the Ge−N linkage formed by dative bonding will keep dimers buckled. In addition, the pyridine molecules are located between the dimer rows.

To decide the most stable configuration for the chemisorption of pyridine, we investigate a large number of the possible configurations having one pyridine molecule (0.25 ML) per $c(4\times2)$ surface unit cell. Here we report the total energy results for all the configurations that are found to be a local energy minimum.

At first, we consider two types of cycloaddition reactions, known as [2 + 2] cycloaddition and [4 + 2] Diels−Alder reactions, which involve one Ge dimer for attachment of a pyridine molecule. For the [2 + 2] cycloaddition, there are several local energy minimum configurations depending on the direction of plane of the aromatic ring or the position of nitrogen of the pyridine molecules: orientation of pyridine molecules to the surface is perpendicular (Figures 1a,b) or parallel (Figures 1c,d). It is found that two [2 + 2] cycloaddition configurations (Figures 1a,b) having trans symmetry are (locally) stable, while some configurations having cis symmetry (not shown here) become unstable. As expected, the surface dimers attached by pyridine molecules become symmetric. Exceptionally, there is a configuration (Figure 1e) where the surface dimer remains buckled (a buckling angle ~7°). The relative energies ΔE (in units of eV/molecule) of the [2 + 2] and [4 + 2] reactions are given in Table 1 with respect to the total energy of the most stable configuration (see Figure 3a) considered in this study.

TABLE 1: Relative Energies ΔE (in eV/molecule) of Cycloaddition-type Configurations of Pyridine on Ge(100)[a]

configuration	C1	C2	C3	C4	C5	C6	C7
ΔE	1.74	1.78	0.67	1.13	0.48	0.59	0.46

[a]The energies ΔE are referred to the total energy of D1 shown in Figure 3a.

TABLE 2: Relative Energies (in eV/molecule) of Bridge-type Configurations of Pyridine on Ge(100)[a]

configuration	B1	B2	B3	B4	B5	B6	B7	B8
ΔE	0.83	0.67	0.73	0.67	0.77	0.42	1.08	0.59

[a]The energy references are same as in Table 1.

TABLE 3: Relative Energies (in eV/molecule) of Dative Bonding Configurations of Pyridine on Ge(100)[a]

configuration	D1	D2	D3
ΔE	0.00	0.14	0.06

[a] The energy references are same as in Table 1.

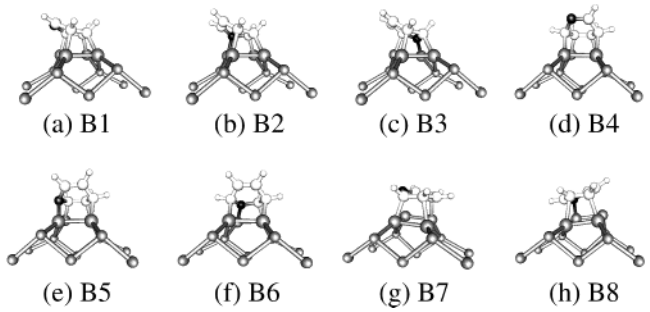

Figure 2. Configurations with the $c(4\times2)$ unit cell at the 0.25 ML pyridine coverage for the so-called bridge (cycloaddition-type) reactions: (a−c) bridge, (d−f) tight bridge, and (g−h) long bridge.

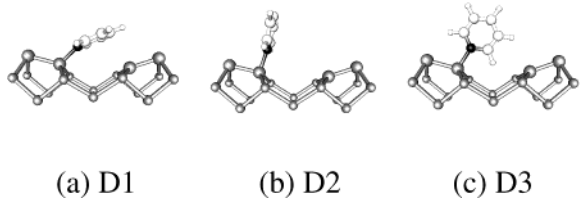

Figure 3. Three configurations with the $c(4\times2)$ unit cell at the 0.25 ML pyridine coverage for the dative-bonding reactions between pyridine molecules and down-Ge atom of Ge dimers.

Note that all the energies shown in the following tables (Tables 2 and 3) are also with respect to this most stable configuration. On the other hand, there are two possible configurations for [4 + 2] Diels−Alder reactions depending on the position of nitrogen. The configuration in Figure 1g is found to be the most stable among cycloaddition reactions considered in Figure 1.

In addition, further likely cycloaddition-type reactions are the formation of "bridges". The formation of bridges involves two Ge dimers.[18] Three types of bridges are possible: so-called bridge, tight-bridge, and long-bridge. There are three configurations for the bridge (Figures 2a−c) and tight-bridge (Figures 2d−f) types, respectively, depending on the position of nitrogen, while two configurations for the long-bridge (Figures 2g,h) type. Their relative energies are given in Table 2. The tight-bridge configuration in Figure 2f is the most stable among all the cycloaddition-type reactions shown in Figures 1 and 2.

So far we have considered all the possible bonding configurations of pyridine molecules located on the Ge dimer row. The

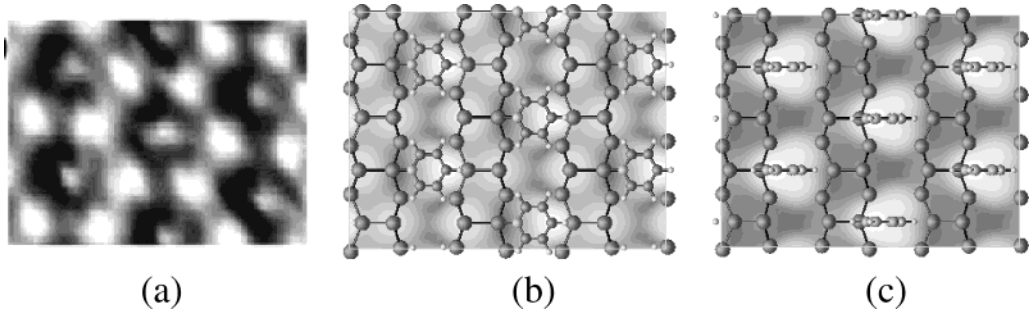

Figure 4. (a) The experimental filled-state image acquired at a bias voltage $V_s = -1.8$ V. (b−c) The theoretical STM images at $V_s = -1.8$ V for two lowest-energy configurations shown in Figures 3a and 3c, respectively. The theoretical filled-state images are overlapped with the top view of the corresponding optimized configurations. The simulated image (b) is found to be very close to the experimental image (a).

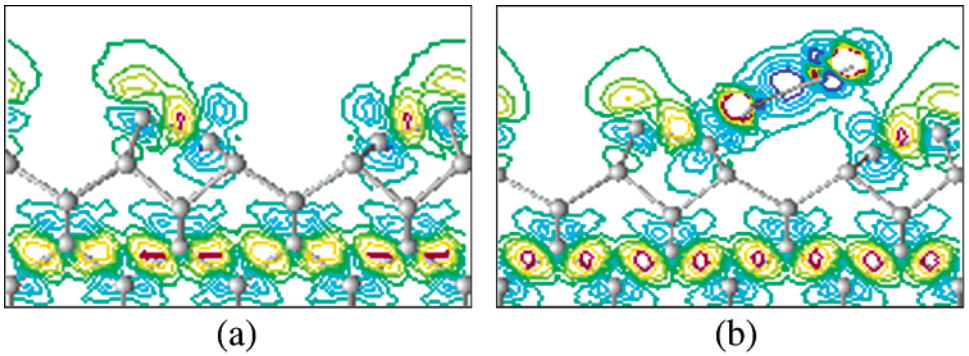

Figure 5. Plot of charge density difference between total valence charge density and a superposition of atomic valence charge densities for (a) clean Ge(100)-*c*(4×2) and (b) pyridine/Ge(100)-*c*(4×2) (see text).

dative bonding configurations resulting from the Lewis acid−base reactions are finally considered, where the pyridine molecules are mainly located between two dimer rows. The electron-deficient down-Ge atom plays a role of a Lewis acid and reacts with the adsorbed pyridine serving as a Lewis base to form a dative bond. There are three configurations depending on the orientation of aromatic ring of pyridine molecule: Figure 3 shows that the orientation of aromatic ring of pyridine molecule is (a) tilted, (b) perpendicular to the Ge surface and parallel to the dimer row, and (c) perpendicular to both the surface and the dimer row. Note that the structures presented in Figure 3 involve two dimers rows for a better view.

Overall, the dative-bonding configurations are much more stable than the configurations resulting from all the cycloaddition-type reactions. Especially, the configuration Figure 3a is the most stable among all the configurations examined in this study. This may imply that the energy gain due to the Ge−N linkage formed by dative bonding is larger than the gain due to formation of cycloaddition-type bonding. The model in Figure 3b is higher in energy by 0.14 eV than that in Figure 3a while the model in Figure 3c is higher by 0.06 eV. From the optimized configuration for the titled configuration (Figure 3a), we find that the Ge−N bond length (2.04 Å) is significantly longer than the experimental covalent bond length (1.70 Å),[8] indicating that pyridine molecule datively binds to the down-Ge atom. The plane of aromatic ring is tilted about 23° with respect to the Ge(100) surface. The adsorption energy for the titled configuration is found to be 2.6 eV per pyridine molecule. It should be noted that the adsorbed pyridine molecules retain their aromaticity.

To explain the experimental filled-state STM images, we simulate the constant-current STM images. The experimental image (Figure 4a) at a bias voltage $V_s = -1.8$ V shows flowerlike protrusions having a hexagonal pattern with regularly arranged dotlike features inside. Note that the dotlike features are on one side in the hexagons. The theoretical STM images are simulated for several bonding configurations having lower energies (not all reported here). We only report the simulation images for the two lowest-energy configurations (Figures 3a and 3c), which are shown in Figures 4b and 4c, respectively, along with the experimental image. The theoretical filled-state images are overlapped with the top view of the optimized adsorption structures. The theoretical STM image in Figure 4b generated from the optimized structure for the titled configuration is very consistent with the experimental STM image, while the simulated image in Figure 4c for the perpendicular configuration does not clearly show the flowerlike spots from the up-Ge atoms around the pyridine molecule shown in the experimental STM images. On the basis of these STM image simulations and energetics, we may exclude the perpendicular configuration from the candidate structures for pyridine-adsorbed Ge(100)-*c*(4×2) showing the experimental image in Figure 4a.

To show the dative bonding character explicitly, we plot the charge density difference $\Delta\rho(\mathbf{r})$, between total valence charge density and a superposition of atomic valence charge densities, for the most stable configuration. Figure 5 gives plots of the charge density differences for (a) the clean Ge(100)-*c*(4×2) surface and (b) the pyridine-adsorbed Ge(100)-*c*(4×2) surface. For the clean Ge(100) surface, the bonding between two Ge atoms in a Ge dimer is clear as shown in Figure 5a. In the $\Delta\rho(\mathbf{r})$ contours there is a pronounced maximum (red color) in the buckled dimer region showing a bonding between two Ge atoms. Above the up-Ge atoms the existence of electron-rich region is explained by a charge transfer from the buckled-down atom to the buckled-up atom. Formation of asymmetric dimers on the clean surface is due to a Jahn−Teller-like distortion from the symmetric configuration. The buckling angle of the dimer is found to be 19.7° and the buckled dimer length is 2.51 Å. The corresponding values by Krüger and Pollmann[19] are 19° and 2.41 Å, while those by Needels et al.[20] are 14° and 2.48 Å.

TABLE 4: Relative Energies (in eV/molecule) of Typical Configurations of Pyridine on Ge(100) and Si(100) with Respect to the Most Stable One on Each Surface

configuration	Ge(100)	Si(100)
dative (tilted) (Figure 3a)	0.00	0.96
dative (perp) (Figure 3c)	0.06	0.94
[2 + 2] (Figure 1c)	0.67	1.75
[4 + 2] (Figure 1g)	0.46	1.03
bridge (Figure 2b)	0.67	0.20
tight-bridge (Figure 2f)	0.42	0.00

After adsorption of pyridine molecules, the charge density difference $\Delta\rho(\mathbf{r})$ is shown in Figure 5b. Similarly to the clean surface, there exist local maxima (orange color) representing a bonding region between two Ge atoms in a dimer and an electron-rich region above the up-Ge atoms. Thus, the buckled-up state of the up-Ge atom still remains but the bonding strength of two Ge atoms may be slightly weaker because the buckled dimer length becomes a little larger to give 2.62 Å. Correspondingly, the buckling angle becomes smaller giving 14.4°. Especially, Figure 5b shows a pronounced maximum (red color) between the down-Ge atom and the pyridine molecule, residing closer to the pyridine molecule. This represents an electron lone pair of nitrogen and thus a dative bonding region. It is concluded that the electron-rich up-Ge atoms maintain the buckled-up state even after adsorption of pyridine.

Finally, it is worthwhile to note that the pyridine-adsorbed Si(100) case is different from the Ge(100) case. From the results of similar calculations for the Si(100) case (see Table 4), a tight-bridge configuration (Figure 2f) is found to be the most stable configuration, which agrees with the results by Tao et al.[18] The theoretical simulation for this tight-bridge configuration can explain the experimental STM images shown on the pyridine-adsorbed Si(100) surface.[21] This is more stable by 0.96 eV than the dative bonding configuration having tilted pyridine (Figure 3a), contrary to the Ge(100) case where the dative bonding configuration is lower in energy by 0.42 eV than the tight-bridge configuration. It is speculated that the difference between the Ge(100) and the Si(100) surfaces mainly comes from the fact that the strength of covalent bond between C and Ge formed by cycloaddition-type reactions is weaker than that between C and Si. Indeed, the Ge−C bond strength was found to be 8.9 kcal/mol (0.49 eV/bond) less than its silicon analogue.[22]

In summary, we have presented results for the pyridine/Ge(100) adsorption configurations resulting from the cycloaddition-type and the Lewis acid−base reactions. It is found that the dative bonding configuration with the adsorbed pyridines tilted has the lowest energy, where pyridine molecules adsorb on the electron-deficient down-Ge atoms of Ge(100). This lowest energy configuration explains the experimental STM images well. It is noted that the difference in the lowest-energy configuration between Ge(100) and Si(100) is due to difference in bond strength of Ge−C and Si−C.

Acknowledgment. This work was supported by grants from the KOSEF through the Center for Nanotubes and Nanostructured Composites, the Brain Korea 21 Project, and the Advanced Backbone IT Technology Development Project of the Ministry of Information and Communication. S.H. acknowledges the support from the KISTI under the fifth Strategic Supercomputing Support Program.

References and Notes

(1) Filler, M. A.; Bent, S. F. *Prog. Surf. Sci.* **2003**, *73*, 1.
(2) Bent, S. F. *J. Phys. Chem.* B **2002**, *106*, 2830.
(3) Bent, S. F. *Surf. Sci.* **2002**, *500*, 879.
(4) Wolkow, R. A. *Annu. Rev. Phys. Chem.* **1999**, *50*, 413.
(5) Hamers, R. J.; Coulter, S. K.; Ellison, M. D.; Hovis, J. S.; Padowitz, D. F.; Schwartz, M. P.; Greenlief, C. M.; Russell, J. N., Jr. *Acc. Chem. Res.* **2000**, *33*, 617.
(6) Lin, Z.; Strother, T.; Cai, W.; Cao, X.; Smith, L. M.; Hamers, R. J. *Langmuir* **2002** *18*, 788.
(7) Solomons, T. W. G.; Fryhle, C. B. *Organic Chemistry*, 7th ed.; Wiley: New York, 2001.
(8) Mui, C.; Han, J. H.; Wang, G. T.; Musgrave, C. B.; Bent, S. F. *J. Am. Chem. Soc.* **2002**, *124*, 4027.
(9) Wang, G. T.; Mui, C.; Tannaci, J. F.; Filler, M. A.; Musgrave, C. B.; Bent, S. F. *J. Phys. Chem. B* **2003**, *107*, 4982.
(10) Cao, X. P.; Hamers, R. J. *J. Am. Chem. Soc.* **2001**, *123*, 10988.
(11) Cho, Y. E.; Maeng, J. Y.; Kim, S.; Hong, S. *J. Am. Chem. Soc.* **2003**, *125*, 7514.
(12) Kresse, G.; Hafner, J. *Phys. Rev. B* **1993**, *47*, R558.
(13) Kresse, G.; Furthmüller, J. *Phys. Rev. B* **1996**, *54*, 11169.
(14) Kresse, G.; Hafner, J. *J. Phys.: Condens. Matter* **1994**, *6*, 8245.
(15) Tersoff, J.; Lang, N. D. Theory of Scanning Tunneling Microscopy. In *Scanning Tunneling Microscopy*; Stroscio, J. A.; Kaiser, W. J., Eds.; Academic Press: Boston, MA, 1993; Methods of Experimental Physics, vol. 27.
(16) Selloni, A.; Carnevali, P.; Tosatti, E.; Chen, C. D. *Phys. Rev. B* **1985**, *31*, 2602.
(17) Tersoff, J.; Hamann, D. R. *Phys. Rev. Lett.* **1983**, *50*, 1998; *Phys. Rev. B* **1985**, *31*, 805.
(18) Tao, F.; Qiao, M. H.; Wang, Z. H.; Xu, G. Q. *J. Phys. Chem.* B **2003**, *107*, 6384.
(19) Krüger, P.; Pollmann, J. *Phys. Rev. Lett.* **1995**, *74*, 1155.
(20) Needels, M.; Payne, M. C.; Joannopoulos, J. D. *Phys. Rev. Lett.* **1987**, *58*, 1765.
(21) Maeng, J. Y. Ph.D. Thesis, 2002.
(22) Mui, C.; Bent, S. F.; Musgrave, C. B. *J. Phys. Chem. A* **2000**, *104*, 2457.